

Nb-Ta Behavior during Magma-to-Pegmatite Transformation Process: Record from Zircon Megacryst in Pegmatite

Authors

Sheng He^{1,*}, Ziying Li¹, Abdullah Al Jehani², Dongfa Guo¹, Zaben Harbi², Yuyan Zhang¹

1. Beijing Research Institute of Uranium Geology, China National Nuclear Corporation, Beijing
100029, China

2. Saudi Geological Survey, Jeddah 21514, Saudi Arabia

Sheng He (First Author, Corresponding Author, *hesheng201410@163.com)

Testing method of major elements composition

Compositional analyses for whole-rock major elements were conducted at the Analytical Laboratory, Beijing Research Institute of Uranium Geology. Major element compositions were determined using a Philips PW2404 X-ray fluorescence (XRF), with analytical precision better than 1%; FeO was measured using the volumetric method.

Nb, Ta content and Nb/Ta ratio of melt

We can use Nb, Ta content, Nb/Ta ratio of zircon and D_{Nb} , D_{Ta} , D_{Nb}/D_{Ta} to calculate Nb, Ta content and Nb/Ta ratio in the melt. The equation is as follows:

$$Nb_{Melt} = \frac{Nb_{Zircon}}{D_{Nb}}$$
$$Ta_{Melt} = \frac{Ta_{Zircon}}{D_{Ta}}$$
$$\frac{Nb_{Melt}}{Ta_{Melt}} = \frac{Nb_{Zircon}}{Ta_{Zircon}} * \frac{D_{Ta}}{D_{Nb}}$$

where Nb_{Melt} , Ta_{Melt} , Nb_{Zircon} , Ta_{Zircon} are the Nb, Ta content in melt and zircon, respectively. D_{Nb} , D_{Ta} are the partition coefficient for Nb, Ta.

Nb, Ta evolution model during fractional crystallization

We assumed that only rutile and titanite fractional crystallization can intensely increase the Nb/Ta ratio in the melt due to low crystallization amount of mica and amphibole and low D_{Nb} , D_{Ta} of feldspar, quartz and pyroxene. Detailed information can be obtained in article. The equation of Nb, Ta Rayleigh fractionation evolution model is as follows:

$$C^l = C_0 * (1-F)^{D-l}$$
$$D = D_{Nb} or D_{Ta} * X$$

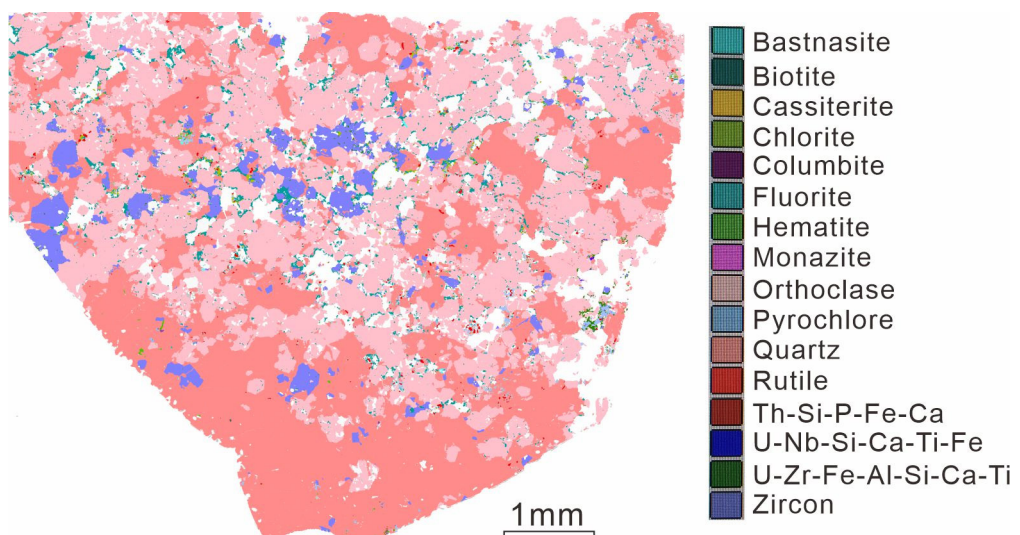
where C are the Nb, Ta content in melt. C_0 are the Nb, Ta concentration in original melt. D_{Nb} , D_{Ta} are the partition coefficient for Nb, Ta. D are the total partition coefficient for Nb, Ta. F means the amount of fractional crystallization. And X means the proportion of rutile or titanite in total crystallization.

Supplementary Figures and Tables

Supplementary Tables S1–S7 are submitted in Excel form, please refer to the electronic form for details.



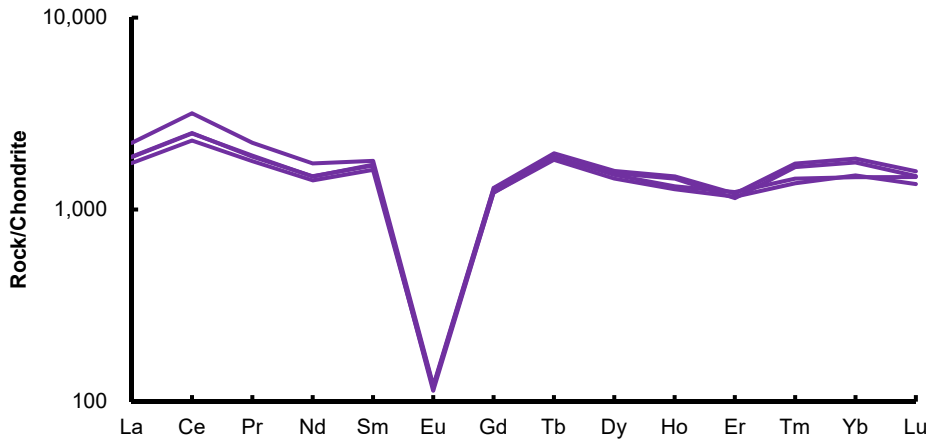
Supplementary Figure S1 Typical outcrop photo of pegmatite.



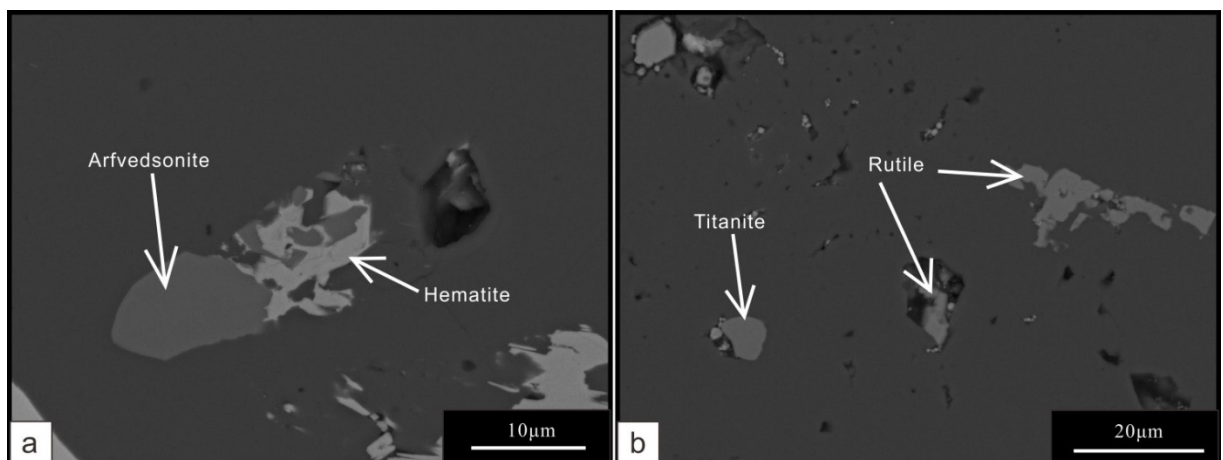
Supplementary Figure S2. AMICS-SEM image of marginal zone of pegmatite. AMICS-SEM means the Advanced Mineral Identification and Characterization System (AMICS)-Automated Mineralogy System-Scanning Electron Microscope (SEM)

Supplementary Table S1 The major elements content of marginal zone of pegmatite (%)

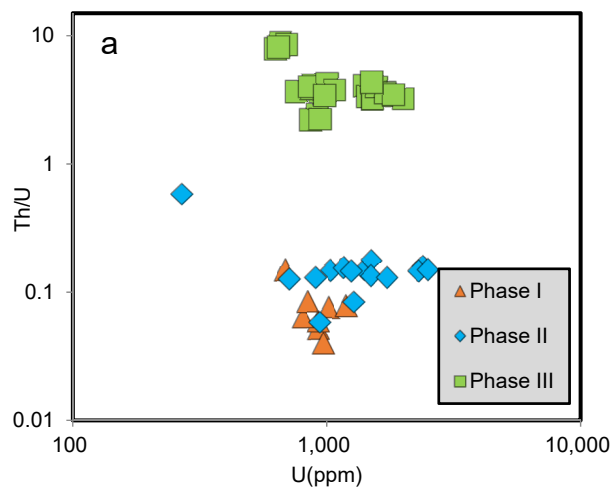
NO.	Sample	SiO ₂	Al ₂ O ₃	Fe ₂ O ₃	MgO	CaO	Na ₂ O	K ₂ O	MnO	TiO ₂	P ₂ O ₅	LOI*	FeO
1	HS-3-1-1	68.54	10.74	4.87	0.335	0.773	0.671	7.01	0.074	0.588	0.052	2.32	0.42
2	HS-3-1-2	68.56	10.67	4.94	0.331	0.781	0.683	7.02	0.075	0.587	0.052	2.31	0.4
3	HS-3-2-1	68.74	10.61	4.86	0.344	0.768	0.677	6.95	0.072	0.587	0.056	2.32	0.39
4	HS-3-2-2	68.75	10.7	4.78	0.334	0.771	0.665	6.97	0.071	0.584	0.058	2.31	0.34

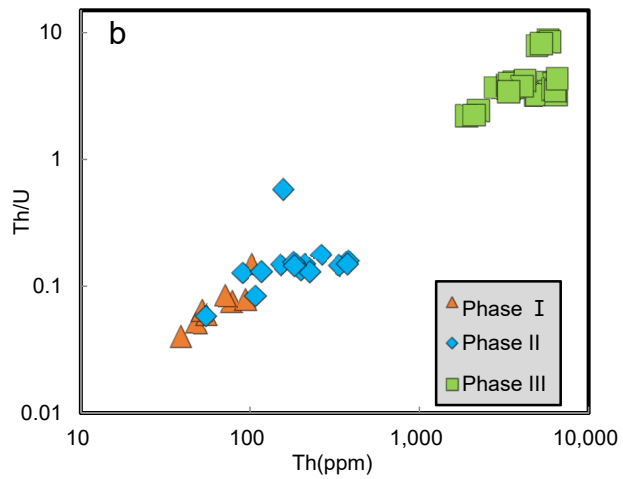


Supplementary Figure S3. Chondrite-normalized REE patterns of marginal zone of pegmatite. The chondrite and primitive mantle values are from McDonough and Sun [1].

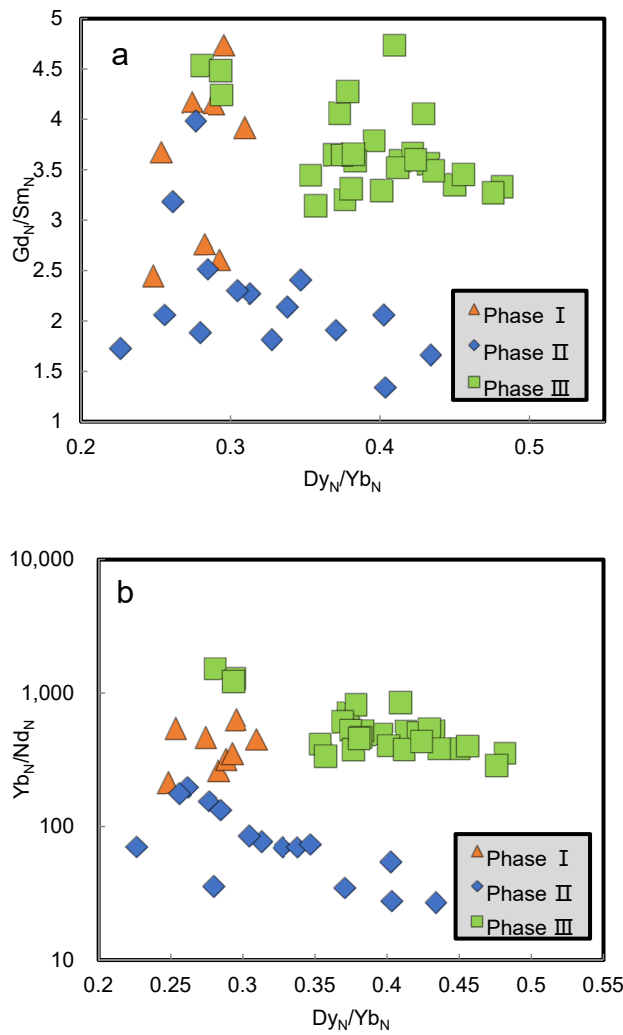


Supplementary Figure S4. Arfvedsonite, hematite, titanite and rutile occur in marginal zone of pegmatite, hematite replaces arfvedsonite, which indicates higher oxygen fugacity in late magma. (a) Arfvedsonite and hematite occur in marginal zone; (b) Titanite and rutile occur in marginal zone.

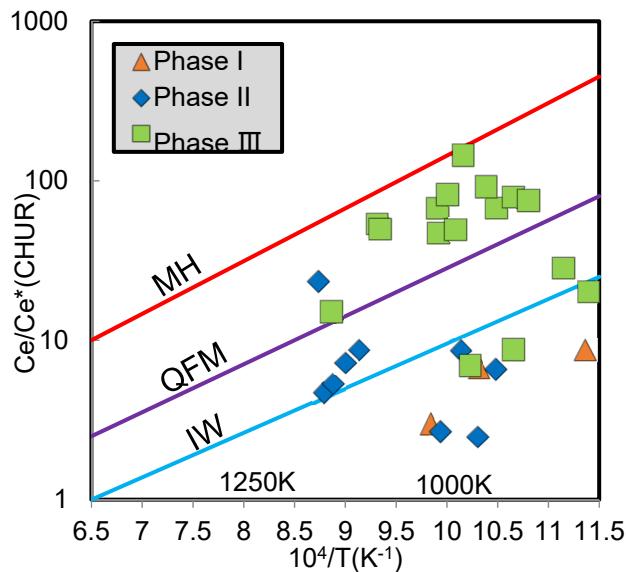




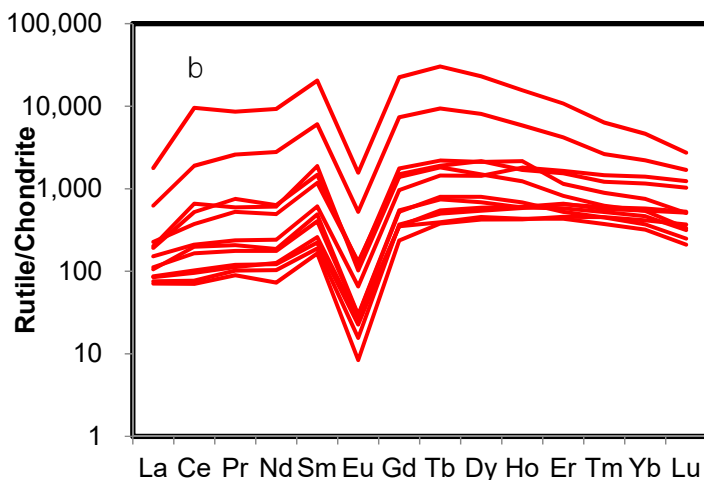
Supplementary Figure S5. Th/U ratios vs U, Th content of Phase I, II, III zircon, Th content and Th/U ratio of Phase III zircon is much higher than those of Phase I, II (**a and b**)



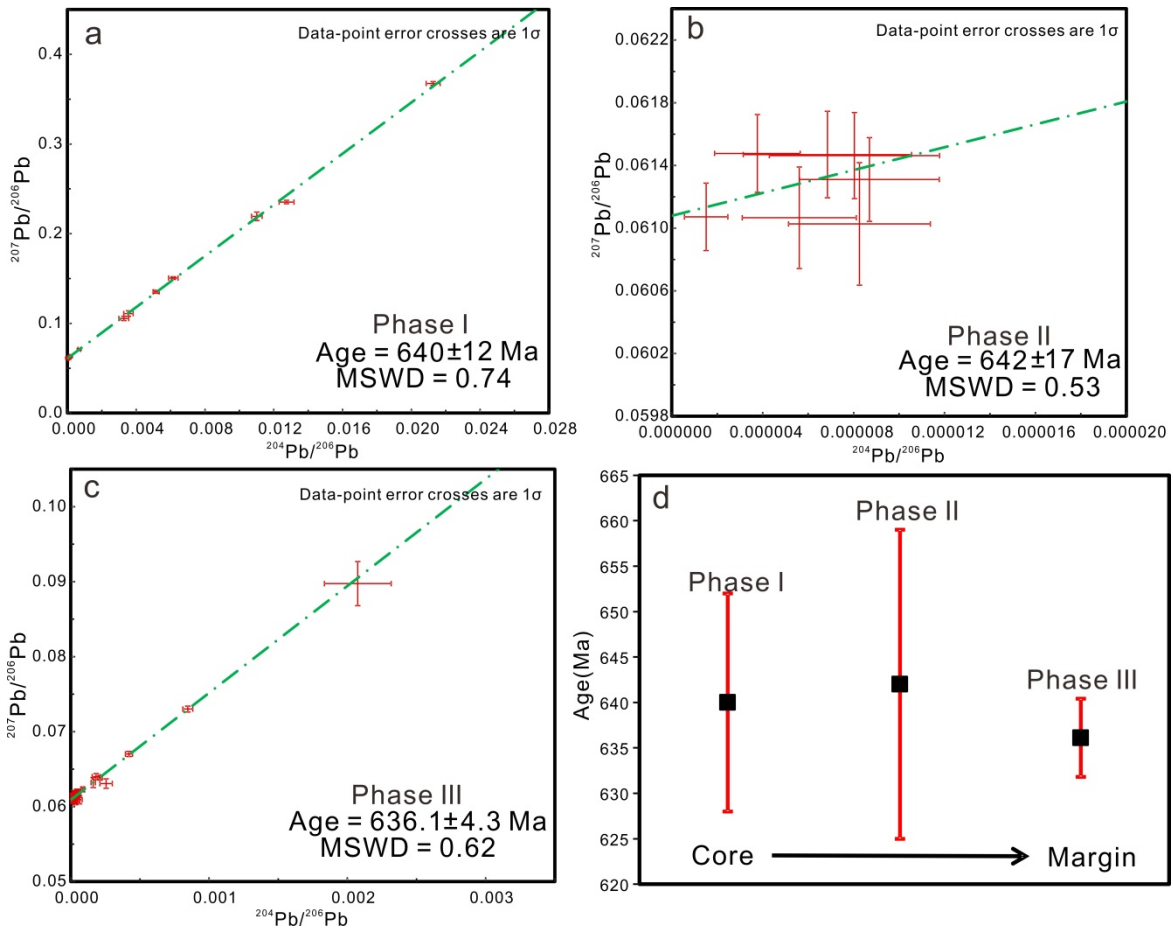
Supplementary Figure S6 REE evolution characteristics of Phase I, II, III in zircon megacryst (**a and b**)



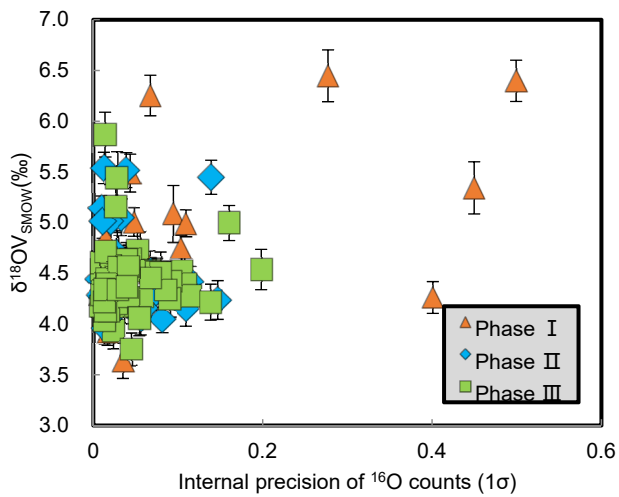
Supplementary Figure S7. Magnitude of Ce anomaly versus $10^4/T$ (K^{-1}) for Phase I, II and III. The Ce anomaly is calculated as $(Ce/Ce^*)_{CHUR} = (Ce_N)/[(La_N \times Pr_N)^{0.5}]$ where La_N , Ce_N , Pr_N are the La, Ce, Pr contents normalized to chondrite [1]. The plot also shows the magnitudes of Ce anomalies in zircon corresponding to several common oxygen fugacity buffers (MH = magnetite-hematite; QFM = quartz-fayalite-magnetite; IW = iron-wüstite). Temperatures of zircon megacryst were calculated by Ti-in-zircon thermometry [2], assuming $a_{SiO_2}=1$, $a_{TiO_2}=1$



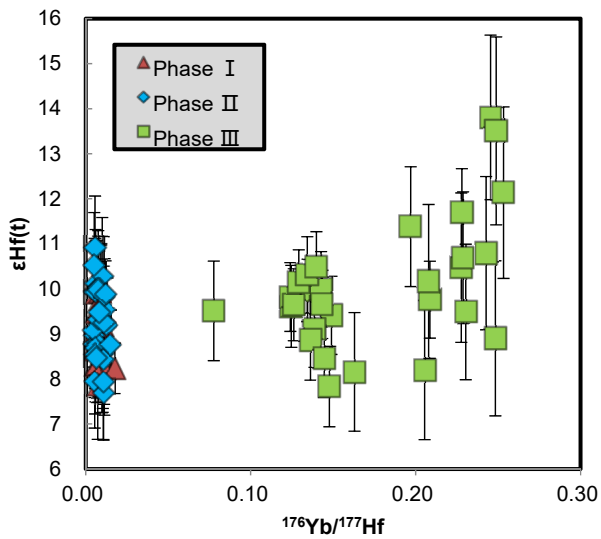
Supplementary Figure S8. REE evolution characteristics of rutile



Supplementary Figure S9. $^{207}\text{Pb}/^{206}\text{Pb}$ - $^{204}\text{Pb}/^{206}\text{Pb}$ isochron for zircon megacryst (phase I to Phase III zircon) (a-d)



Supplementary Figure S10. The $\delta^{18}\text{O}$ value vs internal precision of ^{16}O counts, indicating that >6.0‰ of phase I may result from contamination of mineral inclusions



Supplementary Figure S11. The $^{176}\text{Yb}/^{177}\text{Hf}$ value vs $\epsilon\text{Hf}(t)$, indicating that higher $\epsilon\text{Hf}(t)$ of >12.0 in phase III may result from high Yb content and inaccurate correction of ^{176}Yb . Error bars are 1σ

Supplementary Table S13. Nb, Ta partition coefficient compiled from previous studies

No.	Rock/melt type	D_{Nb}	D_{Ta}	$D_{\text{Nb/Ta}}$	References
1	Synthetic andesitic melt	0.089	0.078	1.14	[3]
2	Coarse-grained hornblende biotite quartz diorite	236			[4]
3		21	6.3	3.33	
4		2.2	2.4	0.92	
5	A-type granitoids	26.5	14.5	1.83	
6		2.62			
7		0.3	0.8	0.38	
8	I-type-magmatic-arc related granitoids	1.9	2.6	0.73	
9		0.3	15.1	0.02	[5]
10	Shoshonitic granodiorites	3.5	3.3	1.06	
11		0.5	1.9	0.26	
12	Quartz monzonites	0.3	1.2	0.25	
13		0.6	0.8	0.75	
14	Ultrapotassic syenogranite	1.6	2.9	0.55	
15	Silicic magma	2.09	1.29	1.62	[6]

Supplementary Table S14. Nb/Ta ratio of melt calculated by zircon Nb/Ta ratio, assuming $D_{\text{Nb}}/D_{\text{Ta}}=3$ and $D_{\text{Nb}}/D_{\text{Ta}}=0.3$

Samples	Zircon phases	Assuming $D_{\text{Nb}}/D_{\text{Ta}}=3$	Assuming $D_{\text{Nb}}/D_{\text{Ta}}=0.3$
z2526-33	Phase I	0.088	0.876
z2526-34	Phase I	0.078	0.775
z2526-35	Phase I	0.045	0.451
z2526-36	Phase I	0.061	0.615

z2526-37	Phase I	0.127	1.274
z2526-38	Phase I	0.111	1.111
z2526-39	Phase I	0.189	1.893
G496-27	Phase I	0.104	1.041
z2526-1	Phase II	0.731	7.311
z2526-2	Phase II	0.671	6.710
z2526-3	Phase II	0.622	6.217
z2526-4	Phase II	0.534	5.337
z2526-5	Phase II	0.472	4.723
z2526-6	Phase II	0.565	5.648
z2526-9	Phase II	0.224	2.237
z2526-29	Phase II	0.167	1.672
z2526-30	Phase II	0.188	1.875
z2526-31	Phase II	0.168	1.681
z2526-32	Phase II	0.436	4.360
z2526-41	Phase II	0.884	8.841
z2526-42	Phase II	0.575	5.747
z2526-44	Phase II	0.363	3.626
G495-13	Phase II	0.481	4.810
z2526-15	Phase III	2.487	24.867
z2526-16	Phase III	2.957	29.571
z2526-19	Phase III	3.292	32.925
z2526-20	Phase III	3.250	32.497
z2526-21	Phase III	3.230	32.302
z2526-22	Phase III	4.516	45.162
z2526-24	Phase III	4.476	44.763
z2526-25	Phase III	2.011	20.112
z2526-26	Phase III	1.888	18.884
z2526-27	Phase III	2.335	23.355
z2526-28	Phase III	2.040	20.397
z2526-50	Phase III	1.972	19.722
z2526-51	Phase III	4.036	40.357
z2526-52	Phase III	4.810	48.099
z2526-53	Phase III	4.431	44.308
z2526-54	Phase III	4.060	40.605
G495-11	Phase III	3.473	34.733
G495-19	Phase III	3.260	32.596
G495-28	Phase III	2.656	26.560
G495-29	Phase III	2.376	23.764
G495-30	Phase III	2.954	29.537
G495-32	Phase III	4.259	42.591
G495-33	Phase III	2.396	23.962
G496-19	Phase III	1.860	18.602
G496-20	Phase III	1.871	18.708

G496-21	Phase III	2.190	21.904
G496-22	Phase III	1.792	17.921

Supplementary Table S15. Nb, Ta content and Nb/Ta ratio of melt calculated by $D_{Nb}=0.08$, $D_{Ta}=0.13$

Samples	Zircon phases	Nb (ppm)	Ta (ppm)	Nb/Ta
z2526-33	Phase I	20	47	0.4
z2526-34	Phase I	24	64	0.4
z2526-35	Phase I	15	68	0.2
z2526-36	Phase I	22	74	0.3
z2526-37	Phase I	31	51	0.6
z2526-38	Phase I	23	42	0.5
z2526-39	Phase I	34	37	0.9
G496-27	Phase I	68	133	0.5
z2526-1	Phase II	906	254	3.6
z2526-2	Phase II	856	262	3.3
z2526-3	Phase II	792	261	3.0
z2526-4	Phase II	2211	850	2.6
z2526-5	Phase II	1689	733	2.3
z2526-6	Phase II	2435	884	2.8
z2526-9	Phase II	1850	789	2.3
z2526-29	Phase II	649	595	1.1
z2526-30	Phase II	965	1184	0.8
z2526-31	Phase II	789	863	0.9
z2526-32	Phase II	825	1007	0.8
z2526-41	Phase II	606	285	2.1
z2526-42	Phase II	452	105	4.3
z2526-44	Phase II	298	106	2.8
G495-13	Phase II	888	502	1.8
z2526-15	Phase III	2656	157	16.9
z2526-16	Phase III	2477	156	15.9
z2526-19	Phase III	623	48	12.9
z2526-20	Phase III	579	50	11.6
z2526-21	Phase III	638	44	14.4
z2526-22	Phase III	1858	89	20.8
z2526-24	Phase III	1656	137	12.1
z2526-25	Phase III	1954	136	14.4
z2526-26	Phase III	1743	109	16.1
z2526-27	Phase III	2162	136	15.8
z2526-28	Phase III	2419	154	15.7
z2526-50	Phase III	1615	138	11.7
z2526-51	Phase III	1776	196	9.1
z2526-52	Phase III	1580	173	9.1
z2526-53	Phase III	1674	157	10.7
z2526-54	Phase III	1566	179	8.7

G495-11	Phase III	1921	87	22.0
G495-19	Phase III	1702	78	21.8
G495-28	Phase III	1656	169	9.8
G495-29	Phase III	671	73	9.2
G495-30	Phase III	674	59	11.4
G495-32	Phase III	1463	147	9.9
G495-33	Phase III	903	94	9.6
G496-19	Phase III	2063	105	19.7
G496-20	Phase III	2141	91	23.4
G496-21	Phase III	2290	106	21.6
G496-22	Phase III	1905	96	19.8

Supplementary References

1. McDonough, W. and S.s. Sun, The composition of the Earth. *Chem. Geol.* **1995**, 120, 3-4, 223-253.
2. Ferry, J.M. and E.B. Watson, New thermodynamic models and revised calibrations for the Ti-in-zircon and Zr-in-rutile thermometers. *Contrib. Mineral. Petr.* **2007**, 154, 4, 429-437.
3. Burnham, A.D. and A.J. Berry, An experimental study of trace element partitioning between zircon and melt as a function of oxygen fugacity. *Geochim. Cosmochim. Acta* **2012**, 95, 196-212.
4. Thomas, J.B., et al., Determination of zircon/melt trace element partition coefficients from SIMS analysis of melt inclusions in zircon. *Geochim. Cosmochim. Acta* **2002**, 66, 16, 2887-2901.
5. Nardi, L.V.S., et al., Zircon/rock partition coefficients of REEs, Y, Th, U, Nb, and Ta in granitic rocks: Uses for provenance and mineral exploration purposes. *Chem. Geol.* **2013**, 335, 1-7.
6. Bachmann, O., M.A. Dungan, and F. Bussy, Insights into shallow magmatic processes in large silicic magma bodies: the trace element record in the Fish Canyon magma body, Colorado. *Contrib. Mineral. Petr.* **2005**, 149, 3, 338-349.